

 Very Important Paper

# A Hairpin Ribozyme Derived Spliceozyme

 Jikang Zhu,<sup>[a]</sup> Robert Hieronymus,<sup>[a]</sup> and Sabine Müller\*<sup>[a]</sup>

The vast majority of RNA splicing in today's organisms is achieved by the highly regulated and precise removal of introns from pre-mRNAs via the spliceosome. Here we present a model of how RNA splicing may have occurred in earlier life forms. We have designed a hairpin ribozyme derived spliceozyme that mediates two RNA cleavages and one ligation event at specific positions and thus cuts a segment (intron) out of a parent RNA and ligates the remaining fragments (exons). The cut-out intron

then performs a downstream function, acting as a positive regulator of the activity of a bipartite DNAzyme. This simple scenario shows how small RNAs can perform complex RNA processing dynamics, involving the generation of new phenotypes by restructuring segments of given RNA species, as well as delivering small RNAs that may play a functional role in downstream processes.

## Introduction


Nature harbors a wide variety of RNA molecules with different structures and functions. Among those, ribozymes have attracted particular attention as key players in a hypothetical RNA world at the origin of life.<sup>[1]</sup> The nowadays known, naturally occurring ribozymes have diverse three-dimensional structures and are divided into several classes according to their size and mechanism.<sup>[2]</sup> Activities of natural ribozymes are mostly related to cleavage and/or ligation of RNA phosphodiester linkages by either transesterification or hydrolysis, and in the special case of the ribosome to peptide bond formation. Although the scope of their reactions is thus relatively limited, ribozymes perform a wide variety of biological tasks.<sup>[3]</sup> They are involved in the replication of circular RNA genomes,<sup>[4]</sup> in the maturation of tRNAs,<sup>[5]</sup> and they play a role in RNA splicing.<sup>[6]</sup> RNA splicing is an important process, where introns are excised from a primary transcript, and the remaining exons become ligated to the mature mRNA, which subsequently is used for translation.<sup>[7]</sup> In eukaryotes, this process is supported by the spliceosome, a large ribonucleoprotein complex formed from five small nuclear RNPs composed of snRNAs and proteins.<sup>[8]</sup> Apart from the spliceosome, there are also self-splicing group I and group II introns, which catalyse their own excision through sequential transesterifications.<sup>[6]</sup> Such self-splicing reactions are observed in genes encoding rRNA, mRNA, and tRNA in various organelles and organisms, from prokaryotes to eukaryotes.<sup>[2b,9]</sup> Whereas group I introns employ an external guanosine as a cofactor,<sup>[10]</sup> group II introns use a specific adenosine within their sequence to initiate the first transesterification step.<sup>[11]</sup> Thus, group II


introns share a common mechanism with the spliceosome, which together with some common architectural features supports the suggestion that group II introns and the spliceosome have a common evolutionary origin.<sup>[12]</sup>

Group I introns have been redesigned to work in trans, whereby they can recognize a splice site on an external substrate RNA and replace the 5'- or 3'-portion of this substrate.<sup>[13]</sup> Moreover, another group I intron derived variant has been shown to recognize two splice sites on a substrate RNA, remove the intron sequence between the splice sites, and join the flanking exons. Accordingly, this variant of a catalytic group I intron was termed spliceozyme, because it is a ribozyme that functions like a spliceosome.<sup>[14]</sup>

The efficiency of self-splicing introns suggests an origin in early life, where RNA organisms may have benefited from splicing events. In particular, splicing allows RNA segments to be restructured and thus has an evolutionary effect by generating new RNA sequences with potentially new functions. Excised segments (introns) as such might also have played a role as regulatory or functional elements in other downstream processes, which is now known to occur in the case of miRNAs or snoRNAs that are often found in introns.<sup>[15]</sup> Self-splicing introns are still rather large complex RNAs and therefore are more likely to have emerged in a later stage of the RNA world. In an early period of RNA based life, more simple RNAs of shorter lengths and less complex structure are more convincing candidates to support RNA processing reactions. Based on its unique cleavage-ligation properties, the hairpin ribozyme<sup>[16]</sup> (Figure 1A) is a superior candidate of a small RNA that can support RNA processing in variable scenarios. It features both activities (cleavage and ligation) required for the process of RNA splicing, and we have previously demonstrated that engineered hairpin ribozyme variants can support RNA recombination and self-splicing.<sup>[17]</sup> With a length of about 50 nt, the hairpin ribozyme is quite small. Moreover, only a small part of its sequence is highly conserved (Figure 1A),<sup>[18]</sup> so it can be easily modified to bind and process different substrates. Hairpin ribozymes harbour a common structural motif, which is highly conserved in different RNA forms in different organisms, including archaea.<sup>[19]</sup> Therefore, it seems plausible that hairpin-

[a] J. Zhu, Dr. R. Hieronymus, Prof. Dr. S. Müller  
 Institute of Biochemistry  
 University of Greifswald  
 Felix-Hausdorff-Strasse 4, 17487 Greifswald (Germany)  
 E-mail: sabine.mueller@uni-greifswald.de

 Supporting information for this article is available on the WWW under <https://doi.org/10.1002/cbic.202300204>

 © 2023 The Authors. ChemBioChem published by Wiley-VCH GmbH. This is an open access article under the terms of the Creative Commons Attribution License, which permits use, distribution and reproduction in any medium, provided the original work is properly cited.

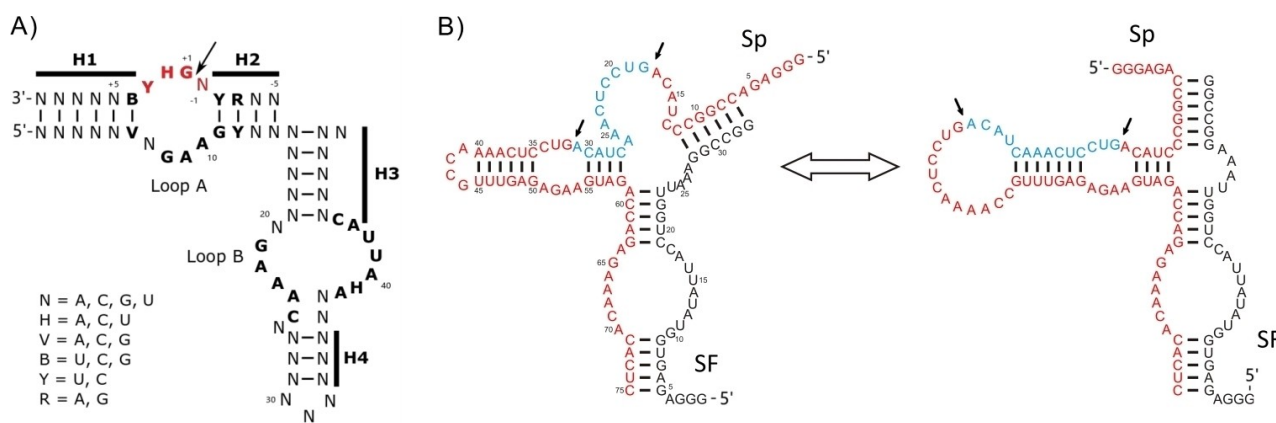


**Figure 1.** A) Consensus sequence of the hairpin ribozyme.<sup>[18]</sup> B) Secondary structure of the engineered spliceozyme in two alternative folds.

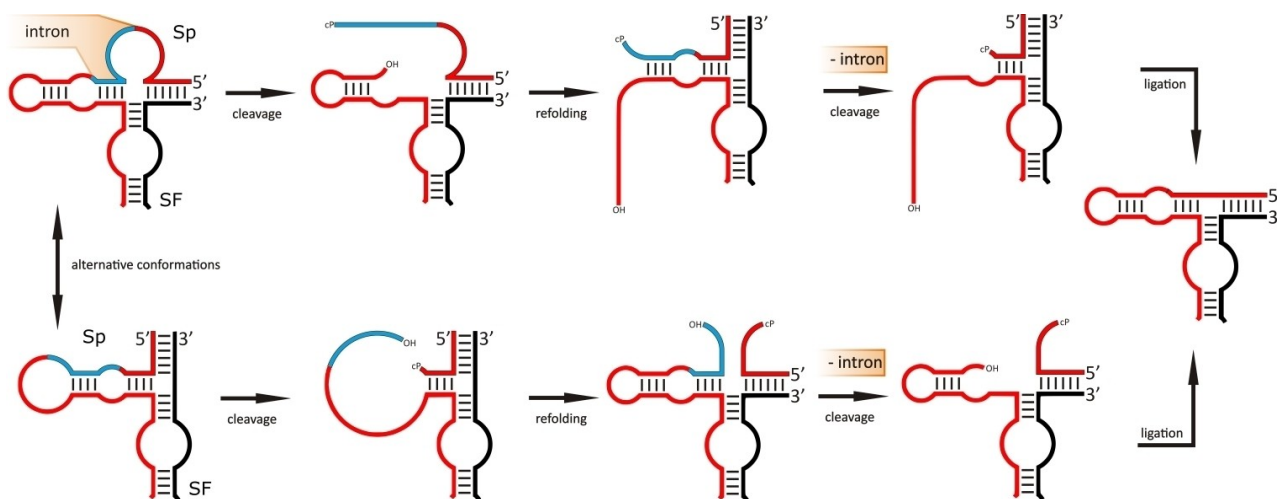
like ribozyme structures have emerged rather early in evolution and that they may have played a role in early life. Here we demonstrate hairpin ribozyme mediated RNA splicing as a possible scenario of RNA processing. We have designed a hairpin ribozyme derived RNA that supports excision of an internal RNA sequence (intron) and ligation of the remaining fragments (exons) in a splicing like reaction. The cut-out intron then performs a functional role in a downstream event, making successful splicing detectable in a functional assay, and moreover, modelling the generation of small regulatory RNAs with downstream functions.

## Results and Discussion

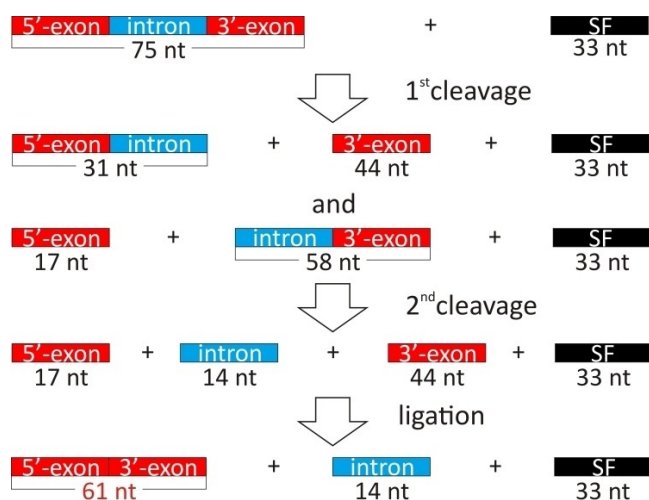
Key to the development of a hairpin ribozyme derived spliceozyme is controlling the equilibrium between the natural reactions of the hairpin ribozyme: RNA cleavage and RNA ligation. As it has been reported in the literature in the past and used in a number of our hairpin ribozyme engineering works,<sup>[17c,20]</sup> the cleavage-ligation equilibrium of the hairpin ribozyme is strongly dependent on the ribozyme structure. Ligation requires the ribozyme being stably folded in a docked conformation, whereas cleavage can proceed also from transiently docked ribozyme-substrate complexes. Hence, hairpin ribozymes that are capable of folding in a stable three-dimensional structure would favor ligation, while hairpin ribozymes that are less stable, however stable enough to form a catalytically competent conformation, would favor cleavage. Taking this into account, we have designed our spliceozyme as shown in Figure 1B. The original hairpin ribozyme consists of four Watson-Crick base-paired helices interrupted by the two loops A and B. Reversible cleavage occurs in loop A between N and G at the N\*GHY site (marked in red in Figure 1A). The full spliceozyme is derived from the hairpin ribozyme, however, composed of two RNA strands: the spliceozyme strand Sp containing the exons and the intron, and the supporting factor strand SF. In order to allow a splicing reaction to occur, we have implemented two A\*GUC sites (according to the N\*GHY

consensus sequence) in the Sp strand, thus mimicking the exon-intron-exon structure. The exon-intron junctions are defined by the two cleavage/ligation sites (Figure 1B, Scheme 1). The Sp strand alone cannot form a catalytically competent conformation, allowing the reaction to be controlled by SF. Only in the presence of SF, the spliceozyme can form an active structure and perform the splicing reaction. Thereby, the intron in Sp (blue part in Scheme 1 and 2) is cut out and the remaining Sp exons (red parts in Scheme 1 and 2) are ligated. The SF remains unchanged.

The intron and exon sequences (Figure 1B, Table S1 and Scheme S1 in SI) of our model spliceozyme were chosen arbitrarily, however keeping in place the conserved sequence motifs of the hairpin ribozyme (Figure 1A).<sup>[16]</sup> In order to perform splicing, the spliceozyme has to support two cleavage events and one ligation with the result of releasing the intron and ligating the two exons. Both, cleavage and ligation, follow the specificity and general mechanism of the hairpin ribozyme as shown in Scheme S2 (SI). The sequence of our spliceozyme was designed to allow folding into two alternative conformations, where either one of the intron-exon boundaries (A\*GUC sites) is positioned in the catalytic center to allow cleavage to proceed (Figure 1B, Scheme 1, S1, SI). Cleavage can occur at the respective site, generating characteristic fragments, one with 5'-OH group and the other with 2', 3'-cyclic phosphate (Scheme 1, Scheme S2, SI). After the first cleavage from either one of the conformations has occurred, the ribozyme can refold into the other conformation, allowing cleavage to proceed at the remaining site (Scheme 1, S1, SI). Independent of the order of cleavage events from both conformations, the result is that the intron is released, and the remaining fragments of Sp (exons), carrying the required functionalities (5'-OH, 2', 3'-cyclic phosphate) become ligated. The presence of the two active conformations is essential for the splicing reaction to occur. It is not important from which conformation the process is started. In both variants, the first cleavage is followed by refolding and a second cleavage that leads to the release of the intron. When the remaining exons are refolded with SF, a hairpin ribozyme structure is again formed, and the exons are joined. The



**Scheme 1.** Reaction scheme and simplified secondary structures of the spliceozyme. The Sp is colored red and blue. Red: 5'- and 3'-exons. Blue: intron. Black: SF. The complete primary and secondary structures are shown in Scheme S1 in the Supporting Information.



**Scheme 2.** Scheme of fragmentation during and after the splicing reaction. Detailed sequences of all the fragments are shown in Table S1 in the Supporting Information.

accuracy of this process depends on the specificity of the hairpin ribozyme and the 5'-OH and 2', 3'-cyclic phosphate termini formed during the reactions. Thus, in all cases, cleavage and ligation occur at A\*GUC sites within loop A. The reaction is driven in the desired direction by control of the stability of the different ribozyme complexes along the reaction pathway. In the two conformations the intron is bound to the opposite strand by four or seven base pairs. This allows fast dissociation upon cleavage and suppression of reverse ligation. On the contrary, the Sp fragments (exons) upon release of the intron and refolding, form a more stable structure with SF and ligation is preferred (Scheme 1, S1, SI).

The splicing reaction can be followed by fragment lengths analysis, as educts and products, and all intermediates have different lengths (Scheme 2). The original RNA substrate Sp (75 nt) in the presence of the supporting factor SF (33 nt) is

cleaved at either of the two junctions to result in the free 3'-exon (44 nt) and the 5'-exon-intron conjugate (31 nt) or alternatively, in the free 5'-exon (17 nt) and the intron-3'-exon conjugate (58 nt). Both intron-exon conjugates can undergo cleavage at the remaining intron-exon junction generating the two exons (17 nt and 44 nt) and the free intron (14 nt). Successful exon ligation would be mirrored in the emergence of a new fragment (61 nt). Thus, simple electrophoresis of the crude reaction mixture through a polyacrylamide gel would indicate if the splicing reaction has proceeded as expected.

For experimental evaluation, the two RNAs Sp and SF were produced by *in vitro* transcription with T7 RNA polymerase. The isolated transcripts were incubated together to allow the splicing reaction to proceed, followed by analysis of the reaction mixture on a polyacrylamide gel and visualization of individual bands by UV shadowing (Figure 2A, S5, SI). Whilst no splicing reaction occurs in the presence of Sp or SF alone (Figure S5, SI, lanes 1 and 2), a total of eight bands was detected when both Sp and SF were incubated together (Figure 2A, S5, lanes 3 and 4, SI), corresponding to the predicted pattern (Scheme 2). Hence, bands were assigned as depicted in Figure 2A to Sp (5'-exon-intron-3'-exon, 75 nt), the ligated exons (5'-exon-3'-exon, 61 nt), the intron-3'-exon conjugate (58 nt), the free 3'-exon (44 nt), SF (33 nt), the 5'-exon-intron conjugate (31 nt), the free 5'-exon (17 nt) and the intron (14 nt). The estimated splicing yield is about 11–13% of the ligated exons (SI).

To further secure this initial result, bands corresponding to the free 5'-exon, the free 3'-exon and SF were isolated from the gel and reincubated, followed by electrophoresis of the crude mixture through a polyacrylamide gel. Because of the much smaller RNA amounts used in this experiment, the gel was stained with SYBR-Gold to visualize RNA bands (Figure 2B). A new band appeared corresponding to the 61 nt product resulting from exon ligation, as concluded from the reference lanes, and hence confirming successful splicing. In a parallel

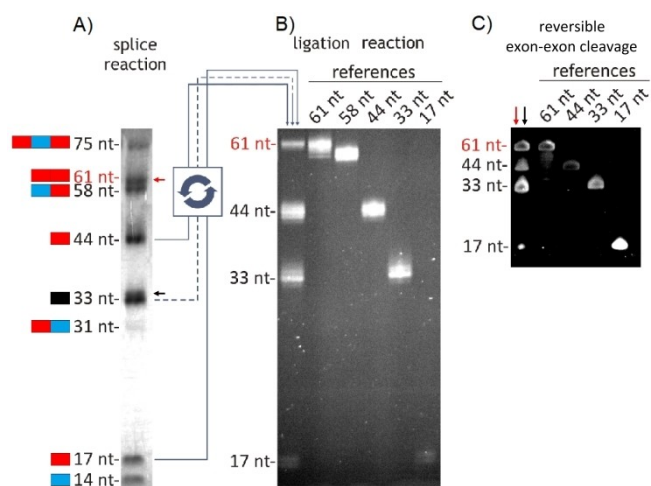
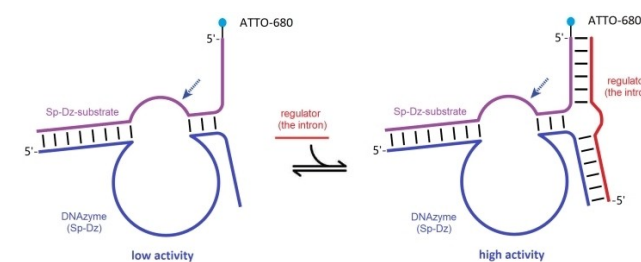


**Figure 2.** A) Denaturing PAA gel (UV shadowing) of the splicing reaction. The gel picture shows the eight expected bands after the splicing reaction. The final product (ligated 5'-exon-3'-exon) has a length of 61 nt. For the color code of fragments see Scheme 2. The full gel picture is shown in Figure S5 in the Supporting Information. Reaction conditions: 50 mM Tris/HCl, 10 mM MgCl<sub>2</sub>, 20 μM Sp, 20 μM SF, 37 °C for 3 h. B) As control, the two exon fragments were isolated from the prior splicing reaction, and the ligation reaction was carried out with the two isolated exons and the SF, resulting in the desired 61 nt ligation product, seen on the denaturing PAA gel with SYBR-Gold staining. Reaction conditions: 50 mM Tris/HCl, 10 mM MgCl<sub>2</sub>, 1 μM 5'-exon, 1 μM 3'-exon, 1 μM SF, 20 °C for 3 h. The five samples acting as references were extracted from the prior splicing reaction. C) The ligated exon fragment was isolated from the prior splicing reaction (red arrow in A), and reincubated with the isolated SF (black arrow in A), resulting in cleavage at the exon-exon junction generating the expected 44 nt and 17 nt cleavage products (lane marked with a red and black arrow). The denaturing PAA gel was stained with SYBR-Gold. Reaction conditions: 50 mM Tris/HCl, 10 mM MgCl<sub>2</sub>, 0.4 μM 5'-exon-3'-exon, 0.4 μM SF, 37 °C for 3 h.

experiment, we isolated the putative exon-exon ligation product from the splicing reaction shown in Figure 2A and reincubated it with SF. Analysis of this reaction clearly showed that reversible exon-exon cleavage occurred, producing both the 17 nt 5'-exon and the 44 nt 3'-exon (Figure 2C). Thus, the identity of the putative exon-exon ligation product was confirmed.

In addition to fragment lengths analysis, we sought a functional test that would underpin successful splicing. We



**Scheme 3.** Design and kinetic modulation of the regulated bipartite DNAzyme variant SP-Dz. Shown is the simplified secondary structure of the DNAzyme variant (blue), the substrate (purple), and the regulator (red). The cleavage site is marked by an arrow. The complete primary and secondary structures are shown in Figure S1 in the Supporting Information.

decided to use a RNA cleaving DNAzyme construct, which requires an external cofactor to fold in a catalytically competent conformation and designed a construct derived from the bipartite DNAzyme developed by Sen and co-workers<sup>[21]</sup> (Scheme 3). The DNAzyme Sp-Dz that we have designed (Scheme 3, Figure S1, SI), is composed of the catalytic strand (blue) and the RNA substrate (purple) bound by Watson-Crick base pairing. In this composition, activity is low, owing to the insufficiently stable conformation. Activity would be increased in the presence of a third strand (regulator, red) that interacts with both the catalytic strand and the substrate, thus stabilizing the active conformation and allowing cleavage of the RNA substrate to proceed. The red regulator strand is the 14 nt intron set free during the splicing reaction (Scheme 2, Figure S1, SI). It acts as a positive regulator of DNAzyme activity by binding simultaneously to Sp-Dz and the substrate, thus forming the catalytically competent complex. Accordingly, an increase in cleavage activity would indicate the presence of the intron and in consequence successful splicing.

To monitor the reaction, the chemically synthesized RNA substrate (Sp-Dz-substrate) was conjugated to the fluorescent dye ATTO680. This way the cleavage reaction can be qualitatively and quantitatively analyzed by gel electrophoresis on a LI-COR plate sequencer and fluorescence detection. First, we carried out control experiments to test the regulatory function of the intron sequence (Figure 3A, B, Figure 4A). The Sp-Dz-

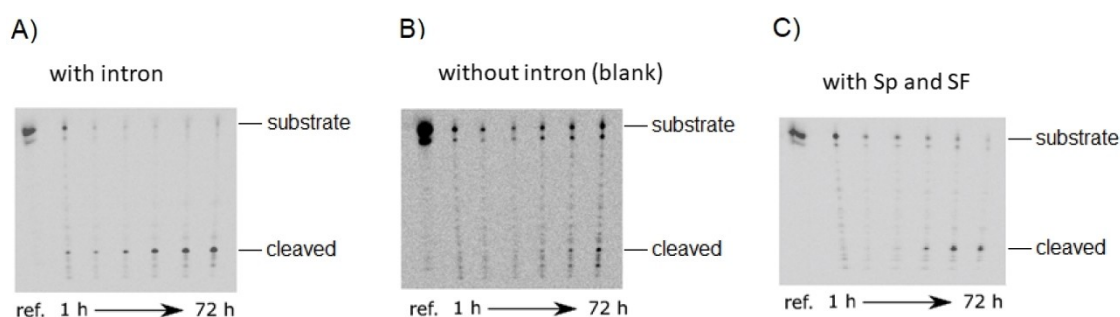


**Figure 3.** A–C) Denaturing PAA gels of the cleavage of the Sp-Dz-substrate by Sp-Dz, visualized by fluorescence detection on the LI-COR sequencer, in the presence of the intron (A); in the absence of the intron (B); in the presence of Sp and SF (C). Reaction conditions: 50 mM Tris/HCl, 1 M NaCl, 200 mM MgCl<sub>2</sub>, 4 nM substrate, 2 μM DNAzyme, 4 μM regulator, 25 °C for 72 h. Reference: Sp-Dz-substrate only.



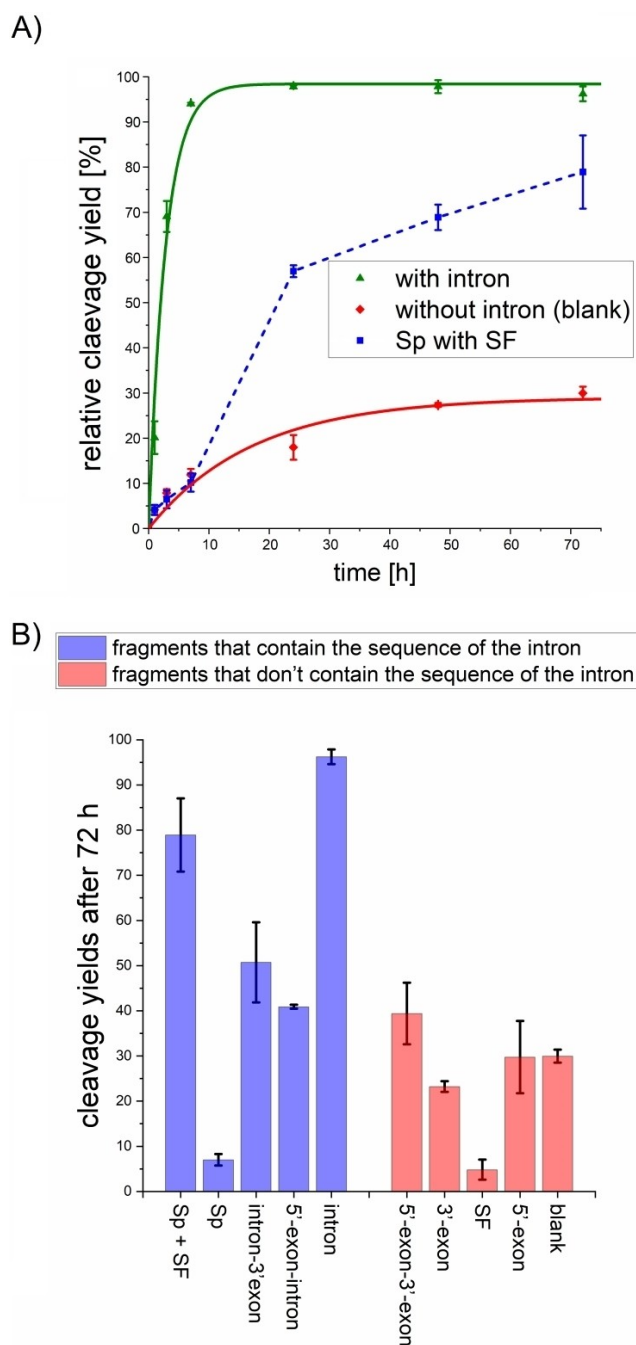


**Figure 4.** A) Kinetic plots of cleavage of the Sp-Dz-substrate by the DNAzyme Sp-Dz in absence (red) and presence (green) of the isolated intron. The cleaved substrate fraction plotted over time was fitted to the equation  $[P] = A(1 - e^{-kt})$ , where  $[P]$  represents the fraction of substrate cleaved at time  $t$ , and  $A$  represents the highest percentage of total RNA cleaved. Data obtained for DNAzyme cleavage in the presence of Sp and SF in a combined assay (blue) were not fitted, because of the more complex kinetics of the combined splicing and cleavage reaction. Average data from three independent measurements have been used. B) Cleavage yields after 72 hours of the Sp-Dz-substrate by DNAzyme Sp-Dz in the presence of different fragments. Average data of three independent measurements were collected. See also Table S2 in the Supporting Information.

substrate was incubated with the DNAzyme Sp-Dz in the presence and absence of the 14 nt intron, isolated from a

preparative splicing reaction. At defined time points (1, 3, 7, 24, 48, and 72 h), aliquots were taken out of the reaction mixture and immediately added to an equal volume of stop-mix (7 M urea, 50 mM EDTA). The samples were subjected onto a polyacrylamide gel and reaction products were quantified by fluorescence detection on the LI-COR sequencer (Figure 3A, B). The positive effect of the intron sequence is clearly seen. Reaction in the presence of the intron is much faster and proceeds with higher efficiency (96% cleaved substrate after 72 h) than reaction in the absence of the intron (30% cleaved substrate, Figure 4A). Thus, the role of the intron sequence as positive regulator of the DNAzyme activity was clearly confirmed.

After this promising result, we next investigated, if the combination of the spliceozyme with the DNAzyme Sp-Dz in one reaction pot results in a similar positive regulation of activity. For this purpose, DNAzyme Sp-Dz and the Sp-Dz-substrate were incubated together with Sp and SF. Cleavage of the substrate was clearly detected and proceeded faster than in the absence of the intron (Figure 3C, 4A). Strikingly, cleavage starts slowly, resembling the cleavage curve in the absence of the intron. The reaction then becomes faster, approaching the level of the reaction in the presence of the isolated intron. This implies that first splicing had to occur to release the intron, which then activates the DNAzyme (Figure 4A). We carried out a set of controls, as the Sp strand also contains the sequence of the intron (not yet spliced) and thus presumably can also regulate the activity of the DNAzyme. We tested Sp, SF, and all intermediate products of the splicing reaction separately as regulators of DNAzyme activity. DNAzyme cleavage reactions were performed as described above in the presence of individual RNA species (Figure S2–S4, Table S2, S1), and the reaction yield after 72 h was used as a measure for the efficacy of the regulator strand (Figure 4B). In the presence of Sp and SF in splicing buffer, DNAzyme activity was found being similarly high (79% cleavage after 72 h) as in the presence of the isolated intron (96%). All other fragments, even if containing the intron sequence (intron-3'-exon and 5'-exon-intron), performed worse (Figure 4B) or even inhibited reaction (Sp or SF alone), confirming the presence of the excised intron in the combined spliceozyme and DNAzyme reaction assay, and thus successful splicing.

## Conclusion

The spliceozyme shown in this work was able to perform a splicing reaction, cutting a defined fragment (intron) out of an RNA sequence and ligating the two truncated terminal fragments (exons), demonstrating that relatively small RNAs with cleavage and ligation activity can support splicing-like reactions. In contrast to our previous work on RNA self-splicing, where a designed hairpin ribozyme structure was shown to act as a self-splicing intron, cutting itself out of an RNA molecule and supporting ligation of the resulting fragments,<sup>[17c]</sup> we here show that a designed hairpin ribozyme variant can also support RNA splicing when it is part of the exon. Interaction of two RNA

strands (Sp and SF, Scheme 1) leads to assembly of the active spliceozyme that mediates the removal of an intron out of one of the two strands and ligates the remaining exons. Thus, it is not the ribozyme, which is spliced out as a catalytic intron, but instead, activity comes from RNA elements located in the two parent RNAs and acting together as spliceozyme. Apart from conserved nucleobases in the two loop structures, the sequence of the hairpin ribozyme is highly flexible, which implies that splicing as demonstrated herein can occur in variable sequence context, making the process highly attractive to early RNA world scenarios. There, it may have played a role in RNA processing dynamics and generation of new phenotypes by restructuring segments of given RNA species. Furthermore, in the same way, as we have shown the excised intron being a functional element in the downstream reaction of a DNAzyme, RNA fragments generated by the action of spliceozymes may have performed new regulatory or other functions in RNA based life. Furthermore, spliceozymes such as those proposed here could find application in research and biotechnology as tools to remove internal RNA sequences and provide them as regulatory elements for selected downstream reactions. However, at present, this process is limited to in vitro applications. For application in cells, issues such as delivery or in situ expression of splicing enzymes, as well as their efficiency and possible off-target effects, would need to be considered.

Overall, the work presented here adds to the collection of rationally designed hairpin ribozyme variants, which mediate complex RNA processing reactions, although having a rather short length and simple structure.<sup>[20]</sup> This is of importance for early life scenarios, where assembly of short RNAs to functional complexes is a convincing scenario. Our spliceozyme composed of two short strands falls exactly in this category.

## Experimental Section

**RNA synthesis:** RNAs were prepared by chemical synthesis or in vitro transcription. Chemical synthesis was performed by the phosphoramidite approach on a Gene Assembler Special DNA/RNA Synthesizer. Phosphoramidite building blocks and supports (CPG) were obtained from ChemGenes. For 5'-terminal labelling of the Sp-Dz substrate with ATTO680, 5'-TFA-Amino Modifier C6-CE Phosphoramidite (Link Technologies Ltd.) was coupled to the 5'-end. For removal of protecting groups after synthesis and release from the support RNAs were incubated with a 1:1 (v/v) solution of 32% ammonia and 8 M ethanolic methylamine at 65 °C for 40 min, followed by lyophilization. The obtained pellets were dissolved in a mixture of 600  $\mu$ l TEA-3HF and 200  $\mu$ l DMF to remove the 2'-O-TBDMS protecting groups. The mixture was incubated at 55 °C for 90 min and the reaction was stopped by the addition of 200  $\mu$ l of water. Upon transfer of the mixture into a Falcon tube, the RNA was precipitated with butanol overnight followed by centrifugation at 6000 rpm for 60 min at 10 °C. The RNA pellet was taken up in gel loading buffer (98% (v/v) formamide; 2% (v/v) 0.5 M EDTA) and subjected onto a 15% denaturing PAA gel. Bands containing the full-length RNA were cut out, the gel pieces were crushed and the RNA was eluted passively with 0.3 M NaOAc (pH 5.4) in three replicates. The combined elution solutions were lyophilized until a concentrated RNA solution was obtained, from which the RNA was precipitated with ethanol. Enzymatic RNA synthesis proceeded by in vitro transcription from 1  $\mu$ M template DNA (biomers.net GmbH)

containing the T7 promotor sequence (TAATACGACT CACTA-TAGGG) in HEPES buffer (20 mM NaHEPES (pH 7.5), 30 mM MgCl<sub>2</sub>, 2 mM spermidine, 40 mM DTT). The transcription mixture was heated to 90 °C for 2 min followed by slow cooling to 37 °C. 2 mM of NTP mix and 0.5 U/ $\mu$ l of T7 RNA polymerase were added and the mixture was incubated at 37 °C for 3–6 h. The obtained RNA was precipitated from ethanol. The pellet was taken up in gel loading buffer (98% (v/v) formamide; 2% (v/v) 0.5 M EDTA) and subjected onto a 15% denaturing PAA gel. Bands containing the full-length RNA were cut out, the gel pieces were crushed and the RNA was eluted passively with 0.3 M NaOAc (pH 5.4) in three replicates. The combined elution solutions were lyophilized until a concentrated RNA solution was obtained, from which the RNA was precipitated with ethanol. For sequences of RNAs see the Supporting Information (Table S1).

**Splicing reaction:** Sp and the SF were added to 50 mM Tris/HCl buffer (pH 7.5). The reaction mixture was denatured at 90 °C for 2 min, cooled down to 37 °C, and incubated at 37 °C for 15 min. Then 10 mM MgCl<sub>2</sub> was added to the mixture to give a final concentration of 20  $\mu$ M of both RNAs in a volume of 120  $\mu$ l. The mixture was incubated for 180 min at 37 °C, followed by ethanol precipitation. The pellet was dissolved in 30  $\mu$ l water and 30  $\mu$ l loading buffer (98% (v/v) formamide; 2% (v/v) 0.5 M EDTA) and subjected onto a 10% denaturing polyacrylamide gel. Bands were visualized by UV shadowing, using Vilber Lourmat and Chemi-Smart 2000 instrumentation.

**Ligation of isolated exons:** The 5'-exon, the 3'-exon, and the SF were added to 50 mM Tris/HCl buffer (pH 7.5). The reaction mixture was denatured at 90 °C for 2 min, cooled down to 20 °C, and incubated at 20 °C for 15 min. Then 10 mM MgCl<sub>2</sub> was added to the mixture to give a final concentration of 1  $\mu$ M of each RNA species in a volume of 10  $\mu$ l. The mixture was incubated for 180 min at 20 °C, followed by the addition of 10  $\mu$ l loading buffer. The entire mixture was subjected onto a 10% polyacrylamide gel on gel. After electrophoresis, the gel was stained with SYBR-Gold.

**Cleavage of the isolated 5'-exon-3'-exon splicing product:** The ligated 5'-exon-3'-exon product was isolated from the splicing reaction and incubated with SF in 50 mM Tris/HCl buffer (pH 7.5). The reaction mixture was denatured at 90 °C for 2 min, cooled down to 37 °C, and kept at 37 °C for 15 min. Then 10 mM MgCl<sub>2</sub> was added to give a final concentration of 0.4  $\mu$ M of each RNA species in a volume of 5  $\mu$ l. The mixture was incubated for 180 min at 37 °C. Then, 5  $\mu$ l loading buffer was added and the entire mixture was subjected onto a 10% polyacrylamide gel. After electrophoresis, the gel was stained with SYBR-Gold.

**ATTO680 labelling:** 5 nmol of amino-modified RNA was dissolved in 50  $\mu$ l of 50 mM NaHCO<sub>3</sub><sup>-</sup> buffer (pH 8.2). 25  $\mu$ g of the ATTO680-NHS ester (ATTO-TEC GmbH) was dissolved in an equal volume of DMF and added to the RNA solution. The mixture was incubated for 3 h at room temperature, followed by precipitation of the RNA from ethanol. The pellet was taken up in 0.1 M triethylammonium acetate buffer (pH 7.5) and the labelled RNA was purified by reversed phase HPLC (ÅKTA purifier; column: 125/4 nucleodur C18; gradient: 5% to 30% acetonitrile in 0.1 M triethylammonium acetate buffer (pH 7.5) over 60 min; flow rate: 0,5 ml/min).

**DNAzyme cleavage:** 0.1 pmol of the ATTO680-labelled substrate of the DNAzyme and 50 pmol of the DNAzyme were mixed in 50 mM Tris/HCl buffer (pH 7.5). The reaction mixture was denatured at 90 °C for 2 min, cooled down to 25 °C, and incubated at 25 °C for 15 min. Then 1 M NaCl, 200 mM MgCl<sub>2</sub>, and 100 pmol of regulator were added to the mixture in a final volume of 25  $\mu$ l. The mixture was incubated at 25 °C. At defined intervals (1, 3, 7, 24, 48, and 72 h), aliquots of the sample were removed and added to an equal

volume of stop-mix (7 M urea, 50 mM EDTA). 0.3 µl of each mix was subjected onto a 10% PAA gel, which was run on a LI-COR4300 DNA sequencer. The labelled RNA species were detected via their fluorescence (700 nm channel). Signal intensities were measured and evaluated with the software Image Studio Lite (LI-COR Bioscience). The fractions of the non-cleaved substrate and the cleavage fragment were determined by the ratio of the individual signal intensities to the sum of the intensities of all bands in the respective lane.

## Acknowledgements

A scholarship from the Landesgraduiertenförderung der Universität Greifswald, awarded to Jikang Zhu is gratefully acknowledged. Open Access funding enabled and organized by Projekt DEAL.

## Conflict of Interests

The authors declare no conflict of interest.

## Data Availability Statement

The data that support the findings of this study are available from the corresponding author upon reasonable request.

**Keywords:** cleavage · hairpin ribozyme · ligation · spliceozyme · splicing

- [1] K. Moelling, F. Broecker, *Int. J. Mol. Sci.* **2021**, *22*.  
 [2] a) W. G. Scott, *Curr. Opin. Struct. Biol.* **2007**, *17*, 280; b) A. Serganov, D. J. Patel, *Nat. Rev. Genet.* **2007**, *8*, 776.  
 [3] a) M. J. Fedor, J. R. Williamson, *Nat. Rev. Mol. Cell Biol.* **2005**, *6*, 399; b) E. Westhof, A. Lescoute, in *Encyclopedia of Virology (Third Edition)* (Eds.:

- B. W. J. Mahy, M. H. V. Van Regenmortel), Academic Press, Oxford, **2008**, pp. 475.  
 [4] a) T. O. Diener, *Proc. Nat. Acad. Sci.* **1989**, *86*, 9370; b) R. Flores, S. Gago-Zachert, P. Serra, R. Sanjuán, S. F. Elena, *Annu. Rev. Microbiol.* **2014**, *68*, 395.  
 [5] C. Guerrier-Takada, K. Gardiner, T. Marsh, N. Pace, S. Altman, *Cell* **1983**, *35*, 849.  
 [6] a) T. R. Cech, *Annu. Rev. Biochem.* **1990**, *59*, 543; b) M. Seetharaman, N. V. Eldho, R. A. Padgett, K. T. Dayie, *RNA* **2006**, *12*, 235.  
 [7] A. F. de Longevialle, I. D. Small, C. Lurin, *Mol. Plant Pathol.* **2010**, *3*, 691.  
 [8] A. I. Lamond, *BioEssays* **1993**, *15*, 595.  
 [9] a) D. Apirion, A. Miczak, *BioEssays* **1993**, *15*, 113; b) A. Hedberg, S. D. Johansen, *Mob. DNA* **2013**, *4*, 17; c) A. Wachter, *Trends Genet.* **2014**, *30*, 172.  
 [10] M. R. Stahley, S. A. Strobel, *Curr. Opin. Struct. Biol.* **2006**, *16*, 319.  
 [11] L. Dai, D. Chai, S.-Q. Gu, J. Gabel, S. Y. Noskov, F. J. H. Blocker, A. M. Lambowitz, S. Zimmerly, *Mol. Cell* **2008**, *30*, 472.  
 [12] C. M. Smathers, A. R. Robart, *Biochim. Biophys. Acta. (BBA) – Gene Regulatory Mechanisms* **2019**, *1862*, 194390.  
 [13] a) P. P. Dotson, 2nd, A. K. Johnson, S. M. Testa, *Nucleic Acids Res.* **2008**, *36*, 5281; b) M. A. Bell, A. K. Johnson, S. M. Testa, *Biochemistry* **2002**, *41*, 15327; c) M. A. Bell, J. Sinha, A. K. Johnson, S. M. Testa, *Biochemistry* **2004**, *43*, 4323; d) D. A. Baum, S. M. Testa, *RNA* **2005**, *11*, 897.  
 [14] Z. N. Amini, K. E. Olson, U. F. Müller, *PLoS One* **2014**, *9*, e101932.  
 [15] D. Rearick, A. Prakash, A. McSweeney, S. S. Shepard, L. Fedorova, A. Fedorov, *Nucleic Acids Res.* **2011**, *39*, 2357.  
 [16] M. J. Fedor, *J. Mol. Biol.* **2000**, *297*, 269.  
 [17] a) R. Hieronymus, S. P. Godehard, D. Balke, S. Muller, *Chem. Commun. (Camb.)* **2016**, *52*, 4365; b) R. Hieronymus, S. Muller, *Ann. N. Y. Acad. Sci.* **2019**, *1447*, 135; c) R. Hieronymus, J. Zhu, S. Muller, *Nucleic Acids Res.* **2022**, *50*, 368; d) R. Hieronymus, S. Muller, *ChemSystemsChem* **2021**, *3*.  
 [18] A. Berzal-Herranz, S. Joseph, B. M. Chowrira, S. E. Butcher, J. M. Burke, *EMBO J.* **1993**, *12*, 2567.  
 [19] N. B. Leontis, E. Westhof, *J. Mol. Biol.* **1998**, *283*, 571.  
 [20] R. Hieronymus, J. Zhu, B. Appel, S. Müller, in *Ribozymes*, **2021**, pp. 439.  
 [21] D. Y. Wang, B. H. Lai, A. R. Feldman, D. Sen, *Nucleic Acids Res.* **2002**, *30*, 1735.

Manuscript received: March 15, 2023  
 Revised manuscript received: May 3, 2023  
 Accepted manuscript online: May 15, 2023  
 Version of record online: June 2, 2023